

Localization of linear kinetic Alfvén wave in an inhomogeneous plasma and generation of turbulence

R. P. Sharma,¹ R. Goyal,^{1,a)} Earl E. Scime,² and N. K. Dwivedi³

¹Centre for Energy Studies, Indian Institute of Technology, Delhi-110016, India

²Department of Physics, West Virginia University, Morgantown, West Virginia 26506-6315, USA

³Austrian Academy of Sciences, Space Research Institute, Schmiedlstrasse 6, 8042 Graz, Austria

(Received 23 December 2013; accepted 2 April 2014; published online 15 April 2014)

This paper presents a model for the propagation of Kinetic Alfvén waves (KAWs) in inhomogeneous plasma when the inhomogeneity is transverse to the background magnetic field. The semi-analytical technique and numerical simulations have been performed to study the KAW dynamics when plasma inhomogeneity is incorporated in the dynamics. The model equations are solved in order to study the localization of KAW and their magnetic power spectrum which indicates the direct transfer of energy from lower to higher wave numbers. The inhomogeneity scale length plays a very important role in the turbulence generation and its level. The relevance of these investigations to space and laboratory plasmas has also been pointed out.

© 2014 AIP Publishing LLC. [<http://dx.doi.org/10.1063/1.4871497>]

I. INTRODUCTION

Alfvén waves are low frequency magnetohydrodynamic (MHD) waves having fundamental importance to laboratory and space plasmas.¹ These were predicted for the first time theoretically by Hannes Alfvén² and observed experimentally by Lundquist.³ Kinetic Alfvén waves (KAWs) are the category of Alfvén waves having a large wave number (k_{\perp}) in transverse direction to the background magnetic field B_0 . The electrons are able to move fast enough to respond adiabatically to the wave fields as the electron thermal speed ($V_{Te} = (k_B T_e / m_e)^{1/2}$) exceeds Alfvén speed (V_A).⁴ Non linear properties of KAWs are of great importance both theoretically⁵⁻⁷ as well as experimentally.⁸ These waves play a significant role in various space phenomena like acceleration of solar wind, coronal heating and dissipation of solar wind turbulence⁹ upon their propagation in space. Goertz¹⁰ has suggested that these waves play an important role in the particle acceleration in nonstationary electric fields. Dissipation of turbulence leads to heating of plasma which in turn is essential to interpret the observations of most astronomical¹¹ and laboratory¹² systems. An important role in the transport of energy into space and astrophysical plasmas is played by MHD turbulence and it is like Kolmogorov¹³ cascade of anisotropic Alfvénic fluctuations.¹⁴ Alexandrova *et al.*¹⁵ observed for the first time the inertial range of Alfvénic fluctuations to be Kolmogorov¹³ like in the magnetosheath. KAWs carry finite perturbations parallel to electric and magnetic fields which cause plasma particles to accelerate and heat up¹⁶ depending on perpendicular wave number. Chaston *et al.*¹⁷ demonstrated that the magnetic fluctuations observed near earth's magnetopause can be described as turbulent spectrum of KAWs. Nykyri *et al.*¹⁸ observed the turbulent spectra in high altitude cusp and revealed that break in observed spectra might be due to damping of obliquely propagating KAWs. Alfvén waves were observed by *Hinode*

spacecraft¹⁹ in 2007. Solar Optical Telescope (SOT) onboard *Hinode*²⁰ also observed upward propagating Alfvén waves. Due to their low frequencies and long wavelengths, these are difficult to observe in laboratory.²¹ Wilcox *et al.*²² verified Alfvén speed ($V_A^2 = B_0^2 / \mu_0 n_0 m_i$) in laboratory plasma experiment. B_0 is background magnetic field, n_0 is background plasma density, and m_i is the ion mass.

In general, space and laboratory plasmas have different kinds of inhomogeneities viz., density fluctuations, temperature, and magnetic field.²³ Xu *et al.*²⁴ theoretically studied the formation of Alfvén solitons in various inhomogeneous systems like magnetosphere, solar wind and interplanetary shocks, etc. Davila²⁵ has given a theoretical approach to study the heating of solar corona by resonant absorption of Alfvén waves by assuming V_A to be background plasma density dependent in transverse direction. Using their experimental approach Gekelman *et al.*²⁶ have depicted the magnetic field variations due to shear Alfvén waves along radial direction in a plasma channel which is having an ambient magnetic field along the length of the plasma channel. Vincena *et al.*²⁷ have studied the variation in Alfvén wave energy along radial direction in an inhomogeneous plasma. But the present study is motivated by a recent experiment by Houshmandyar and Scime⁴ on the propagation of linear KAW in inhomogeneous plasmas and the generation of fluctuating magnetic and electric fields.

In the present study of propagation of low frequency linear KAW through inhomogeneous plasma, we first study semi-analytically for paraxial approximation and then numerically for non paraxial approximation in order to observe the focusing and defocusing of KAW and its energy decay using a power spectrum. For inhomogeneous plasma, V_A gets modified due to recasting of background plasma density profile. The inhomogeneity introduced by plasma density gradient transverse to the background magnetic field²⁸ is incorporated in the present study. The situation is almost similar to laser beam propagating through a fiber optics

^{a)}Electronic mail: ravig.iitd@gmail.com

channel having dielectric constant given by²⁹ $\varepsilon = 1 + \frac{c^2}{V_A^2}$, where c is the velocity of light in free space and V_A is the phase velocity of the wave. As V_A is a function of background plasma density n_0 therefore, V_A gets modified due to inhomogeneity in the density. As a consequence of this modification, the dielectric constant forms a maximum at the centre of the channel and goes on decreasing on moving from core towards the cladding (i.e., along transverse direction). Due to the variation in refractive index (dielectric constant) of the medium, lens like structures are formed and a laser beam propagating through these regions of varying refractive index, gets focused and defocused on regular intervals in space. In fiber optics channel, it is the laser beam which gets self-focused due to change in the refractive index of the medium and in the present case, the KAW beam gets self focused due to inhomogeneous plasma property.

In Sec. II, we have given the detailed dynamics of KAW using paraxial approximation to study the formation of filamentary structures of KAW semi-analytically in intermediate— $\beta(m_e/m_i \ll \beta \ll 1)$ plasma. In Sec. III, numerical technique has been described to solve the dynamical equation of KAW without using paraxial approximation and the conclusions and results have been detailed in Sec. IV.

II. KINETIC ALFVÉN WAVE (KAW) DYNAMICS

Consider an inhomogeneous magnetized plasma having magnetic field \vec{B}_0 in z direction and inhomogeneity in x direction having a density profile $n_0 \exp(-x^2/L^2)$, where n_0 is background plasma density, L is the transverse inhomogeneity scale length. The low frequency KAW having finite amplitude is considered to be propagating along x - z plane. Following the standard method^{30–32} and using Maxwell's equations, continuity equation and equation of motion, the dynamical equation for KAW can be written as

$$\frac{\partial^2 B_y}{\partial t^2} = -(V_{Te}^2 \lambda_e^2 + V_A^2 \rho_i^2) \frac{\partial^4 B_y}{\partial x^2 \partial z^2} + V_A^2 \exp\left(\frac{x^2}{L^2}\right) \frac{\partial^2 B_y}{\partial z^2}, \quad (1)$$

where $V_{Te} = \sqrt{T_e/m_e}$ is electron thermal speed, $V_{Ti} = \sqrt{T_i/m_i}$ is ion thermal speed. $T_e(T_i)$ is the temperature of electron (ion). $\lambda_e = \sqrt{c^2 m_e / 4\pi n_0 e^2}$ is the collisionless inertial length of electrons, $\rho_i = V_{Ti} / \omega_{ci}$ is ion gyroradius, ω_{ci} being ion cyclotron frequency. Before proceeding further for the numerical simulation, we obtain the physical insight by using semi-analytical approach and applying paraxial approximation. For this, we approximate Eq. (1) as

$$\frac{\partial^2 B_y}{\partial t^2} = -(V_{Te}^2 \lambda_e^2 + V_A^2 \rho_i^2) \frac{\partial^4 B_y}{\partial x^2 \partial z^2} + V_A^2 \left(1 + \frac{x^2}{L^2}\right) \frac{\partial^2 B_y}{\partial z^2}. \quad (2)$$

Equation (2) is solved within paraxial approximation ($x \ll r_0 f_0$).³³ r_0 is the scale size of the KAW in transverse direction and f_0 being a dimensionless parameter, represents the beam width of KAW. Substituting the envelope solution

$$B_y = \tilde{B}_0(x, z) e^{i(k_0 x + k_{0z} z - \omega_0 t)} \quad (3)$$

into Eq. (2), the KAW equation can be expressed in the form

$$-2ik_{0z} \frac{\partial \tilde{B}_0}{\partial z} - \frac{k_{0z}^2}{V_A^2} \left(V_{Te}^2 \lambda_e^2 + V_A^2 \rho_i^2 \right) \frac{\partial^2 \tilde{B}_0}{\partial x^2} + k_{0z}^2 \left(\frac{x^2}{L^2} \right) \tilde{B}_0 = 0, \quad (4)$$

where it is assumed that $\partial_z \tilde{B}_0 \ll k_{0z} \tilde{B}_0$, $\partial_x \tilde{B}_0 \gg k_{0x} \tilde{B}_0$ and k_{0x} (k_{0z}) is the component of the wave vector perpendicular (parallel) to $\hat{z} B_0$. ω_0 is the frequency of the KAW.

We now introduce an additional eikonal S_0 to separate Eq. (4) into real and imaginary parts by assuming the solution

$$\tilde{B}_0 = \tilde{A}_0(x) \exp\{ik_{0z} S_0(x, z)\}. \quad (5)$$

Then, the solution of the real part is given by³¹

$$\begin{aligned} \tilde{A}_0^2 &= \frac{\tilde{B}_{00}^2}{f_0} \exp\left(\frac{-x^2}{r_0^2 f_0^2}\right), \\ S_0 &= \varsigma \frac{x^2}{2} + \phi_0, \\ \varsigma &= a \frac{1}{f_0} \frac{df_0}{dz}, \end{aligned} \quad (6)$$

where in Eq. (6), $a = \{(\rho_i^2 + \rho_s^2) k_{0z}^2\}^{-1}$, $\rho_s = c_s / \omega_{ci}$ is the ion gyroradius at electron temperature, $c_s = \sqrt{T_e / m_i}$ is the ion sound speed and the governing differential equation of KAW beam width parameter f_0 is given by

$$\frac{d^2 f_0}{dz^2} = \frac{1}{a^2 R_d^2 f_0^3} - \frac{f_0}{a L^2}, \quad (7)$$

where $R_d = k_{0z} r_0^2$.

The right hand side of Eq. (7) shows the competition between the terms coming from diffraction and inhomogeneous plasma profile. The self-trapping mode occurs by balancing the two terms on the right hand side of Eq. (7). In that case the wave neither converges nor diverges (i.e., $f_0 = 1$) as it propagates along z . This is obtained at a critical inhomogeneity scale length ($L^2(cr) \sim a R_d^2$). In order to illustrate the results, the typical laboratory plasma parameters⁴ used for semi-analytical approach and numerical simulation are: $B_0 \approx 560$ G, $n_0 \approx 10^{13}$ cm⁻³, plasma density $\approx 6 \times 10^{12}$ cm⁻³, $T_e = 81$ 200 K, $T_i = 2900$ K. Using these values, the other parameters obtained are: $\beta \approx 0.002$, $V_A \approx 5 \times 10^7$ cm/s, $V_{Te} \approx 1.1 \times 10^8$ cm/s, $V_{Ti} \approx 4.89 \times 10^5$ cm/s, $c_s = 2.6 \times 10^6$ cm/s, $\omega_{ci} = 5.36 \times 10^6$ rad/s, $\lambda_e = 0.2171$ cm, $\rho_i \approx 0.0912$ cm, $\rho_s \approx 0.483$ cm, $k_{0x} \approx 0.85$ cm⁻¹, $k_{0z} \approx 0.025$ cm⁻¹ for $\omega_0 / \omega_{ci} = f_0 / f_{ci} = 0.4$, $a = 6.6 \times 10^3$, $\omega_0 = 2.14 \times 10^6$ rad/s, $R_d = 10$ cm for $r_0 = 20$ cm. It should be mentioned here that Houshmandyar and Scime⁴ have used helium plasma for their experimental set up but in our theoretical model we have used hydrogen plasma while taking into consideration ion species.

We solved Eq. (7) numerically using boundary conditions corresponding to a plain wavefront viz., $df_0/dz = 0$ and $f_0 = 1$ at $z = 0$. It is observed from Eq. (7) that in case the normalized inhomogeneity scale length of plasma channel has lesser value than its critical value ($L^2(cr) \sim a R_d^2$) there is the

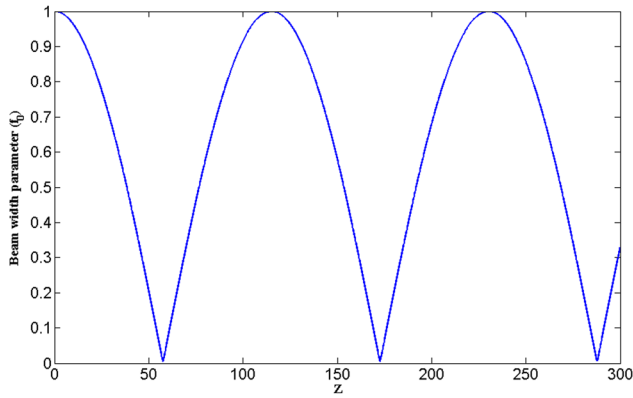


FIG. 1. The variation of beam width parameter (f_0) of KAW along the direction of propagation (z), where z is normalized by R_d .

domination of second term on right hand side over the first term. In that case, the value of beam width f_0 reduces continuously with the stretch along propagation direction till the first term, i.e., diffraction term starts dominating. This results into formation of an intensity maximum at the point where f_0 has a minimum value. Following this, due to domination of diffraction term, there is a continuous increase in the value of f_0 till the second term starts dominating. The process repeats regularly and we get peaks of KAW beam width parameter f_0 . These structures at different locations along the direction of propagation are exemplified in Fig. 1.

III. NUMERICAL SIMULATIONS

We have employed numerical simulation approach to study the filamentation process without paraxial approximation. For this, after using Eq. (3) in Eq. (1), we get in steady state

$$\frac{-2i \partial \tilde{B}_0}{k_{0z} \partial z} - \frac{(V_{Te}^2 \lambda_e^2 + V_A^2 \rho_i^2)}{V_A^2} \frac{\partial^2 \tilde{B}_0}{\partial x^2} + \tilde{B}_0 \exp\left(\frac{x^2}{L^2}\right) - \tilde{B}_0 = 0, \quad (8)$$

where $\partial_z \tilde{B}_0 \ll k_{0z} \tilde{B}_0$ and $\partial_x \tilde{B}_0 \gg k_{0x} \tilde{B}_0$. Equation (8) is normalized and is written in dimensionless form as

$$i \frac{\partial B}{\partial z} + \frac{\partial^2 B}{\partial x^2} + \left(1 - \exp\left(\frac{x^2}{\zeta^2} \varphi\right)\right) B = 0, \quad (9)$$

where $\varphi = x_n^2 / \lambda_x^2$ is a constant and the normalizing parameters are $x_n = \sqrt{(V_{Te}^2 \lambda_e^2 + V_A^2 \rho_i^2)} / V_A$, $z_n = 2 / k_{0z}$ and $\zeta = L / \lambda_x$ is normalized inhomogeneity scale length of the plasma channel, λ_x is the wavelength of KAW in transverse direction. Using the parameters defined above, we found that $x_n \approx 0.486$ cm and $\lambda_x \approx 7.40$ cm for $k_{0x} \approx 0.85$ cm⁻¹. If we look at Eq. (9) critically, it can be solved by using the algorithm developed for solving Non Linear Schrödinger (NLS) equation. Because if we replace the last term in Eq. (9) by

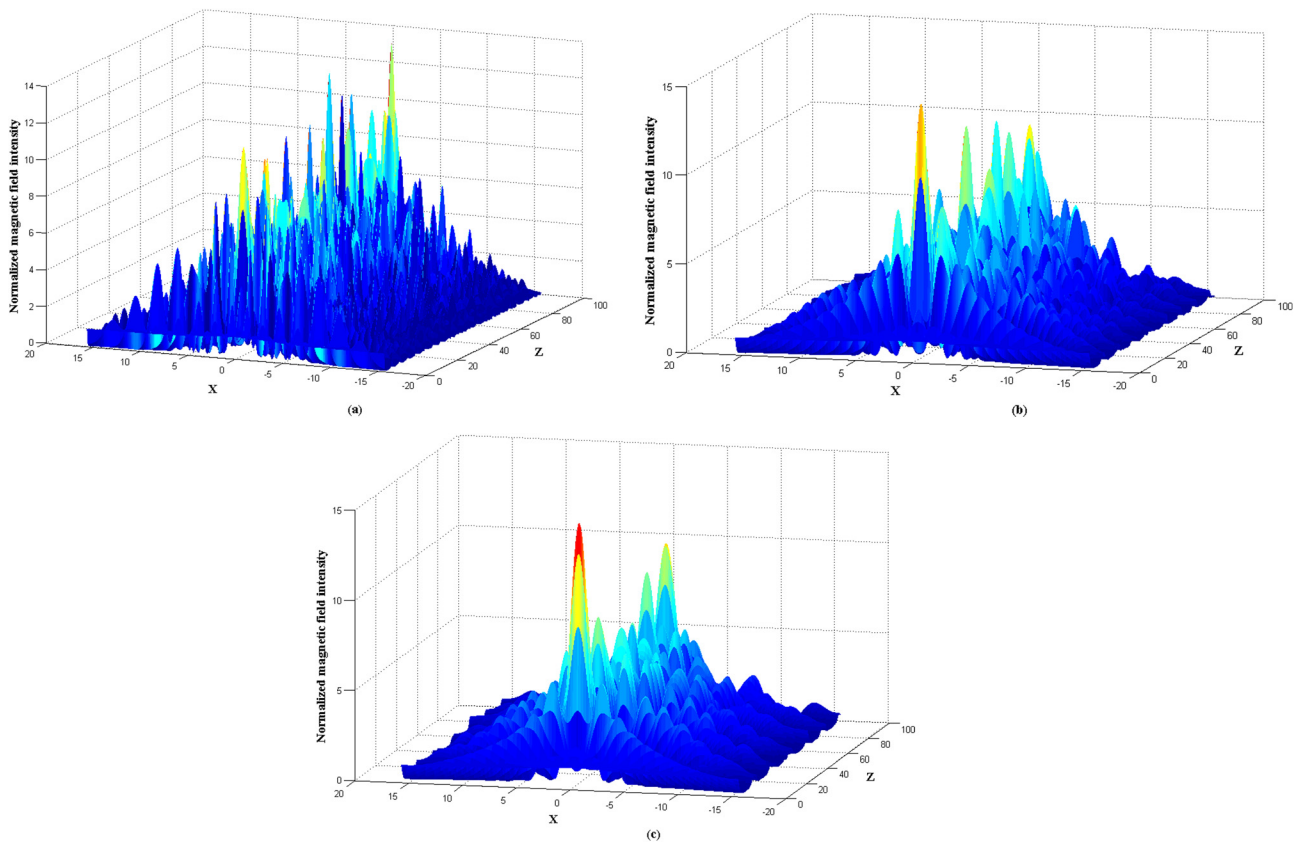


FIG. 2. (a) Normalized magnetic field intensity variation of KAW with direction of propagation (z) and transverse direction (x) for inhomogeneity scale length, $\zeta = 0.6$, where z and x are normalized as defined for Eq. (8) to obtain Eq. (9). (b) Normalized magnetic field intensity variation of KAW with direction of propagation (z) and transverse direction (x) for inhomogeneity scale length, $\zeta = 0.8$, where z and x are normalized as defined for Eq. (8) to obtain Eq. (9). (c) Normalized magnetic field intensity variation of KAW with direction of propagation (z) and transverse direction (x) for inhomogeneity scale length, $\zeta = 0.9$ where z and x are normalized as defined for Eq. (8) to obtain Eq. (9).

$(BB^*)B$, Eq. (9) is NLS equation. Therefore, we first tested the invariants of NLS upto 10^{-5} accuracy. After testing the algorithm for NLS, we modified it for the present case viz. for solving Eq. (9). We considered the perturbation having Gaussian profile on plain uniform KAW and solved Eq. (9) numerically considering the initial condition as

$$B(x, 0) = a_0(1 + \varepsilon \exp(-x^2/r_{10}^2)), \quad (10)$$

where a_0 is the initial value of the amplitude of the homogeneous KAW, ε is the magnitude of perturbation, and r_{10} is the scale size of the perturbation in transverse direction to the propagation.

$a_0 = 1$, $\varepsilon = 0.1$, and $r_{10} = 5$ are chosen as parameters to control the dynamics of evolution. For transverse (x -direction) space integration, we employ the pseudo-spectral method with a periodic length $l_x = r_{10}$. For direction of propagation (z -direction), a finite difference method along with a predictor-corrector scheme has been used. Invariants of NLS equation such as plasmon number $N = \sum_k |B_k|^2$ are monitored to the desired accuracy using a fixed step size in z ($\Delta z = 5 \times 10^{-5}$) for 256 grid point spatial resolution.

The magnetic field filamentary structures with different intensity at different locations are observed along the direction of propagation as well as in transverse direction using above parameters and specifications for a fixed value of l_x . We have also observed the magnetic field fluctuations represented by a power spectrum. In Fig. 2, the magnetic field intensity profile of KAW is illustrated in which the normalized magnetic field intensity is varying with x and normalized distance of propagation z for different values of inhomogeneity scale lengths. The filaments with different intensities along z and x are observed which is obvious as when a small perturbation is imposed on KAW propagating through an inhomogeneous plasma medium, the perturbation draws energy from the main KAW, grows and results into localized structures.

Figs. 2(a)–2(c) show normalized magnetic field intensity profile of KAW for different values of inhomogeneity scale lengths. From the figures, it is clearly observed that as we increase the inhomogeneity scale lengths, the magnetic field fluctuations go on decreasing. This is expected also if we look at the simplified (paraxial) model as given by Eq. (7). By increasing the value of inhomogeneity scale length L , the second term in Eq. (7) will decrease. This will increase f_0 to a large value and hence the normalized magnetic field intensity will decrease and we can infer from the trend that at very large values of inhomogeneity scale length, the system becomes nearly homogeneous.

In Fig. 3, the power spectrum of the magnetic field is shown as $|B_k|^2$ varying along k . This spectrum is obtained using the numerical approach described in Sec. III. We have studied $|B_k|^2$ against k for a fixed value of l_x . We observe that the level of turbulence decreases as we move on higher inhomogeneity scales. Also, the spectra in Figure 3 have been plotted along with Kolmogorov scaling ($k^{-5/3}$) in the revised manuscript. The initial part of the spectra appears to be following nearly Kolmogorov scaling for highest ζ but in other cases there is some deviation from Kolmogorov scaling.

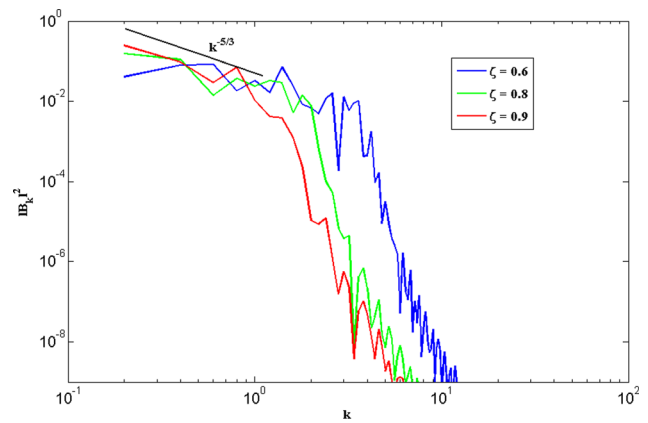


FIG. 3. Variation of $|B_k|^2$ against k for KAW showing the levels of turbulence for different inhomogeneity scales.

It should be mentioned here that the present model is limited to steady state only. Therefore, the localization is in spatial domain and the fluctuations are in wave number domain. We are planning to extend this model to include the temporal effects. This improved model is expected to give insight into the physical mechanism of the origin of fluctuations as observed by Houshmandyar and Scime.⁴

IV. CONCLUSION

We have studied the localization of KAW in an inhomogeneous plasma when the inhomogeneity is transverse to the background magnetic field. The KAW beam breaks up into very high intensity filamentary structures. It is concluded that the perturbation present in KAW may lead to filamentation. Along with this, the competition between the terms coming from diffraction and inhomogeneous plasma profile of KAW may lead to development of turbulence. From these results, we conclude that this model may be a starting point for understanding of the origin of fluctuations observed in laboratory plasma. Not only this, the inhomogeneity incorporated in the present work may be helpful in understanding of various processes taking place in space like solar wind and solar coronal heating. The inhomogeneity along with non-linearity in the plasma medium will be incorporated in the future work which may be quite helpful to study these phenomena.

ACKNOWLEDGMENTS

This work was partially supported by DST (India) and ISRO (India) under RESPOND program.

¹C. Watts and J. Hanna, *Phys. Plasmas* **11**, 1358 (2004).

²H. Alfvén, *Nature* **150**, 405 (1942).

³S. Lundquist, *Nature* **164**, 145 (1949).

⁴S. Houshmandyar and E. Scime, *Phys. Plasmas* **18**, 112111 (2011).

⁵P. Agarwal, P. Varma, and M. S. Tiwari, *Astrophys. Space Sci.* **345**, 99 (2013).

⁶M. Dobrowolny, *Phys. Fluids* **15**, 2263 (1972).

⁷A. Baronia and M. S. Tiwari, *J. Plasma Phys.* **63**, 311 (2000).

⁸P. K. Shukla and L. Stenflo, *Phys. Scr.* **T60**, 32 (1995).

⁹C. C. Chaston, T. D. Phan, J. W. Bonnell, F. S. Mozer, M. Acuna, M. L. Goldstein, A. Balogh, M. Andre, H. Reme, and A. Fazakerley, *Phys. Rev. Lett.* **95**, 065002 (2005).

- ¹⁰C. K. Goertz, *Planet. Space Sci.* **32**, 1387 (1984).
- ¹¹C. S. Salem, G. G. Howes, D. Sundkvist, S. D. Bale, C. C. Chaston, C. H. K. Chen, and F. S. Mozer, *Astrophys. J. Lett.* **745**, L9 (2012).
- ¹²T. A. Carter and J. E. Maggs, *Phys. Plasmas* **16**, 012304 (2009).
- ¹³A. Kolmogorov, *Dokl. Akad. Nauk SSSR* **30**, 301 (1941).
- ¹⁴G. G. Howes, W. Dorland, S. C. Cowley, G. W. Hammett, E. Quataert, A. A. Schekochihin, and T. Tatsuno, *Phys. Rev. Lett.* **100**, 065004 (2008).
- ¹⁵O. Alexandrova, C. Lacombe, and A. Mangeney, *Ann. Geophys.* **26**, 3585 (2008).
- ¹⁶A. Hasegawa and L. Chen, *Phys. Rev. Lett.* **35**, 370 (1975).
- ¹⁷C. Chaston, J. Bonnell, J. P. McFadden, C. W. Carlson, C. Cully, O. Le Contel, A. Roux, H. U. Auster, K. H. Glassmeier, V. Angelopoulos, and C. T. Russell, *Geophys. Res. Lett.* **35**, L17S08, doi:10.1029/2008GL033601 (2008).
- ¹⁸K. Nykyri, B. Grison, P. J. Cargill, B. Lavraud, E. Lucek, I. Dandouras, A. Balogh, N. Cornilleau-Wehrin, and H. Reme, *Ann. Geophys.* **24**, 1057 (2006).
- ¹⁹R. Erdélyi and V. Fedun, *Science* **318**, 1572 (2007).
- ²⁰J.-S. He, C.-Y. Tu, E. Marsch, L.-J. Guo, S. Yao, and H. Tian, *Astron. Astrophys.* **497**, 525 (2009).
- ²¹W. Gekelman, *J. Geophys. Res.* **104**, 14417, doi:10.1029/98JA00161 (1999).
- ²²J. M. Wilcox, F. I. Boley, and A. W. DeSilva, *Phys. Fluids* **3**, 15 (1960).
- ²³H. H. Chen and C. S. Liu, *Phys. Rev. Lett.* **37**, 693 (1976).
- ²⁴T. Xu, B. Tian, L. Li, X. Lu, and C. Zhang, *Phys. Plasmas* **15**, 102307 (2008).
- ²⁵J. M. Davila, *Astrophys. J.* **317**, 514 (1987).
- ²⁶W. Gekelman, S. Vincena, D. Leneman, and J. Maggs, *J. Geophys. Res.* **102**, 7225, doi:10.1029/96JA03683 (1997).
- ²⁷S. Vincena, W. Gekelman, and J. Maggs, *Phys. Rev. Lett.* **93**, 105003 (2004).
- ²⁸R. L. Lysak, *Phys. Plasmas* **15**, 062901 (2008).
- ²⁹F. F. Chen, *Introduction to Plasma Physics and Controlled Fusion* (Springer, 2008).
- ³⁰A. Shukla and R. P. Sharma, *J. Atmos. Sol.-Terr. Phys.* **64**, 661 (2002).
- ³¹P. K. Shukla and L. Stenflo, *Phys. Plasmas* **6**, 4120 (1999).
- ³²P. K. Shukla, L. Stenflo, and R. Bingham, *Phys. Plasmas* **6**, 1677 (1999).
- ³³S. A. Akhmanov, A. P. Sukhorukov, and R. V. Khokhlov, *Sov. Phys. Usp.* **10**, 609 (1968).